Applied Surface Science 330 (2015) 148–157

Contents lists available at ScienceDirect

Applied Surface Science

journal homepage: www.elsevier.com/locate/apsusc

Continuous adsorption of Pb(II) and methylene blue by engineered graphite oxide coated sand in fixed-bed column

Ji-Lai Gong[a,*], Yong-Liang Zhang[a], Yan Jiang[a], Guang-Ming Zeng[a,*], Zhi-Hui Cui[a], Ke Liu[a], Can-Hui Deng[a], Qiu-Ya Niu[a], Jiu-Hua Deng[a], Shuang-Yan Huan[b]

[a] College of Environmental Science and Engineering, Key Laboratory of Environmental Biology and Pollution Control, Ministry of Education, Hunan University, Changsha 410082, China
[b] State Key Laboratory for Chemo/Biosensing and Chemometrics, College of Chemistry and Chemical Engineering, Hunan University, Changsha 410082, China

ARTICLE INFO

Article history:
Received 27 April 2014
Received in revised form 13 October 2014
Accepted 11 November 2014
Available online 20 November 2014

Keywords:
Graphite oxide
Pb(II)
Methylene blue
Adsorption
Fixed-bed column

ABSTRACT

The mixture of several effluents, caused by the improper handling and management of effluents, generated multi-component wastewater containing both metals and dyes, leading to the complicated treatment process. In this study, a continuous adsorption of Pb(II) and methylene blue (MB) has been studied in single and binary solutions by using graphite oxide coated sand (GO-sand) as an adsorbent in a fixed-bed column. GO-sand was analyzed by X-ray photoelectron spectroscopy before and after analyte adsorption. Compared with sand filter, adsorption quantity and capacity for Pb(II) and MB by GO-sand filter were greatly increased. In Pb(II) and MB single solutions, the experimental parameters were investigated in detail including initial concentration, flow rate, bed depth and pH. Exhaustion time decreased with increasing initial concentration and flow rate, and increased with increasing bed depth and pH. In the Pb(II)-MB binary solution, exhaustion time significantly decreased for Pb(II) adsorption, but increased for MB adsorption. The reason was explained that the more favorable adsorption for MB onto the surface of GO-sand than that for Pb(II), which was derived from π–π interaction between MB and GO on sand surface in packed filter. The Yoon–Nelson model was applied at different concentration of Pb(II) and MB to predict the breakthrough curves. The experimental data were well fit with the model indicating that it was suitable for this column design.

1. Instruction

Waste-water discharged from industries increases immensely with the fast developing economy and threats not only environment but also the health of human being. Heavy metal pollution is discharged from those industries such as mining, textiles, painting, hydrometallurgical, electroplating, tinning, refining, pesticides and dyeing [1,2]. Their effluent, usually discharged into aquatic ecosystems untreated or partially treated, mainly contains Cr(III, VI), As(III, V), Cd(II), Pb(II), Cu(II), Zn(II) and Hg(II) [2]. It is well known that excessive Pb(II) will damage the central nervous system, kidney, hemopoiesis, heart and blood vessels and internal secretion system of human beings [2]. Especially for children, Pb(II) even has a permanent damage to their mentality, intelligence, behavior and development, which is non-repairable.

In recent years, the usage of dyes increased in the industries such as plastic, textile, dye, dyestuffs, rubber, paper, leather, cosmetics, food, carpet and printing wastewater extensively [3,4]. Most of dyes including anionic, cationic, non-ionic and zwitterionic and cationic dyes are poisonous [5]. Methylene blue (MB) can cause vomiting, diarrhea, shock, cyanosis, jaundice, quadriplegia and human tissue necrosis [5]. In addition, exposure to dyes will impede light transmission, decrease transparency of waters, retard photosynthetic activity and inhibit the growth of biota [3]. Furthermore, it is hard to biodegrade due to its synthetic and complex aromatic molecular structure [6].

Some researchers have reported that the dye effluent discharged from such industries like textile dyeing, paints and pigments paper manufacturing and automobile production were found along with heavy metals [7,8]. The reason of metals co-existed with dyes in wastewater was partly contributed to metals used as catalysts during the manufacture of some dyes and impurities into dye

* Corresponding authors. Tel.: +86 731 88822829; fax: +86 731 88822829.
E-mail addresses: jilaigong@gmail.com (J.-L. Gong), zgming@hnu.edu.cn (G.-M. Zeng).

http://dx.doi.org/10.1016/j.apsusc.2014.11.068
0169-4332/

molecule [9]. Additionally, the mixture of several effluents due to the improper handling and management of effluents generated multi-component wastewater containing both metals and dyes, leading to the complicated treatment process [7,8]. However, few efforts have been made to remove metals and dyes simultaneously [10]. Therefore, it is necessary to investigate the removal efficiencies for both metals and dyes in co-pollutant solution.

Numerous technologies such as reduction, ion exchange, evaporation, reverse osmosis, precipitation, co-precipitation/adsorption, chemical precipitation and filtration, have been widely applied and developed for removal of Pb(II) and MB[1,2]. However, they suffer from high cost, low efficiency, incomplete metal removal, high reagent and energy requirements and generation of secondary pollution [1,11,12]. Adsorption has the merits of high efficiency, cost-effective, simple operation and environmental friendliness [13]. In previous studies, many adsorbents have been reported such as carbon nanotubes [14], activated carbon, ash, zeolites, metal oxides, chitosan and agricultural byproducts [15]. Olanipekun et al. [2] studied the removal of lead by graphite oxide. Fan et al. [13] reported the lead removal by water-dispersible magnetic chitosan/graphene oxide composites. Graphite oxide nanoparticle (GO-NP) was also used as adsorbent for the removal of MB [5]. Yang et al. [16] studied the adsorption of MB with graphene oxide.

Since its discovery in 2004, the graphene-based materials have created a lot of achievements in many fields. Graphite oxide (GO) containing many functional groups is a popular and potential two-dimensional nanomaterial, which possesses many advantages including dispersibility and affinity to many pollutants in water, large specific surface area, low density, and high adsorption capacity [5,17]. However, it is difficult to pack GO nanomaterial in a column test because it is easy to be washed away and hard to separate for recycling. Hence, a support material is necessary to immobilize GO in a fixed-bed test. Sand is a good choice for its low-cost, chemical stability and availability. Moreover, it also helps to enhance the surface area of GO to get a higher adsorption capacity. GO-sand was prepared with Hummers method using graphite powder as main raw material with low-cost [18]. Sand was fetched from the beach of Xiang jiang river (Changsha, China), which was cheap and available in large quantity. Therefore, this method that GO-sand filter in fixed-bed column for heavy metal and dye removal has the potential to be commercialized. Lee et al. [19] reported the treatment of Pb(II) from aqueous solutions by iron oxide nano-particles-immobilized-sand material in column studies and achieved better results. Eisazadeh et al. [20] investigated the adsorption of Pb(II) in column experiment by iron oxide coated sand, and the removal percentage of Pb(II) reached more than 90%. In previous paper [21], ferrihydrite-coated sand was used as adsorbent in column experiment for the removal of arsenic with a rapid process of adsorption. In this study, GO coated on sand (GO-sand) was employed as adsorbent for the removal of Pb(II) and MB in fixed-bed experiments. Experimental parameters including initial concentration, bed depth, flow rate and pH were investigated. Moreover, the adsorption of binary solutions containing Pb(II) and MB were studied for comparison with that of Pb(II) and MB alone. Both Pb(II) and MB were efficiently removed by GO-sand filter in fixed-bed column and MB removal was enhanced with the presence of Pb(II).

2. Materials and methods

2.1. Chemicals and regents

All the chemicals and regents used in the study were of analytical grades. Lead nitrate ($Pb(NO_3)_2$, 99%) and methylene blue (MB) were dissolved in ultrapure water. Graphite powder (C, 99.85%), hydrogen peroxide (H_2O_2, 30%), potassium permanganate ($KMnO_4$), sodium nitrate ($NaNO_3$) and concentrated sulfuric acid (H_2SO_4, 98%) were used to prepare GO. The initial solutions pH was adjusted by 0.1 M sodium hydroxide (NaOH, 96%) and 1 M hydrochloric acid (HCl, 37%) solutions.

2.2. Preparation of adsorbent

GO was prepared according to the modified Hummers method [22]. Firstly, 1 g graphite powder was added into a conical flask containing 23 mL H_2SO_4 and 0.5 g $NaNO_3$. Secondly, 3 g $KMnO_4$ was added slowly under ice bath condition and stirring. Then, the reaction was maintained at 35 °C for 1 h in water bath. Subsequently, 46 mL ultrapure water was added and the reaction was controlled at 98 °C for 15 min. After reaction, the mixture was diluted to 140 mL with warm water (about 30 °C), followed by the addition of 2.5 mL H_2O_2. Finally, the product (GO) was washed with ultrapure water for several times and dried in freeze for 48 h. The sand was collected from the beach of Xiang jiang river (Hunan, China). Firstly, it was sieved out the same size with a 60 mesh sieve, washed with tap water, soaked with 10% HCl for 6 h, and then, washed with ultrapure water and dried in a drying oven.

GO-sand, the adsorbent used in this study, was prepared by coating GO on the surface of sand according to the previous papers with some modification [23]. Dried and clean sand (10 g) was put in a Petri dish, with 5 mL 0.35 wt% GO dispersion using ultrapure water, and heated up to 150 °C in a drying oven for 2 h [23]. The process was repeated again to increase the GO-coating thickness on sand. The sand was weighted before and after GO coating to quantified the amount of GO coated on sand. The results showed that 0.024 g GO was coated on 10 g sands.

2.3. XPS analysis

The analysis of elements and function groups on the surface of adsorbent were determined using X-ray photoelectron spectroscopy (XPS, Thermo Scientific Escalab 250Xi) with a Mg Kα X-ray source (1254 eV of photons). The high-resolution scans were performed over the 280–300 eV and 525–545 eV ranges (C1s and O1s spectra) for samples before and after lead and MB adsorption, respectively, and additionally, over the 130–155 eV range (Pb4f) and 156–176 eV, 190–210 eV, 390–412 eV ranges (S2s, Cl2p and N1s spectra, respectively) after adsorption. The software Avantage (Thermo Scientific, America) was used to analyze the obtained XPS spectra peaks.

2.4. Preparation of solutions

All of the solutions used in this study were prepared in a set of 1000 mL flasks. The flasks were used for dissolving $Pb(NO_3)_2$ (0.1, 0.2 and 0.3 g) and MB (0.05, 0.1 and 0.2 g) as concentrations of 100 mg/L, 200 mg/L, 300 mg/L and 50 mg/L, 100 mg/L, 200 mg/L, respectively. The pH of Pb(II) and MB solutions was adjusted to 3.19, 4.10, 4.93 and 2.51, 4.21, 8.66, respectively, using 1 M HCl and 0.1 M NaOH solutions.

2.5. Fixed-bed column adsorption studies

The experiments were conducted in a 2 cm diameter and 30 cm length glass column at 25 °C. Four parameters including initial concentration, flow rate, bed depth and pH were studied in the column tests. Glass wool was used as support at the bottom of column to avoid GO-sand being washed away. Column was packed with GO-sand (50, 75 and 100 g) with different bed depth (10, 15 and 20 cm). The influent solution with given flow rate (1, 2 and 3 mL/min) was pumped from the bottom to the top of column by a peristaltic pump

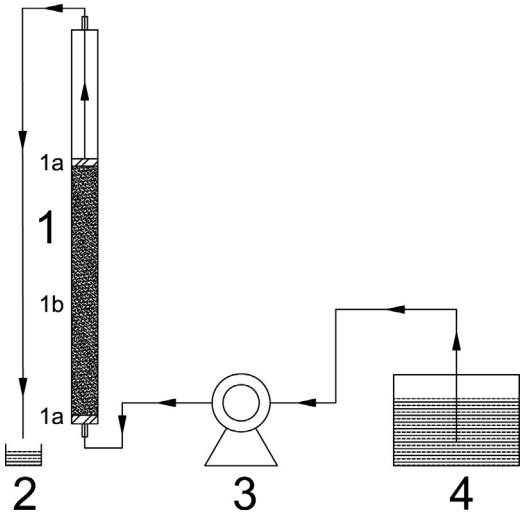

Fig. 1. Schematic diagram of the experimental setup for fixed-bed column studies: (1) fixed-bed column, which contains glass wool and GO-sand indicated by 1a and 1b, (2) effluent solution, (3) peristaltic pump and (4) influent solution.

(shown in Fig. 1). According to preliminary experiment, the effluent of Pb(II) solution was sampled at regular intervals of 10 min and the samples of MB were withdrawn every 20 min. Both of Pb(II) and MB were diluted 100 times for further analyzed. Pb(II) was analyzed by atomic adsorption spectroscopy (AAS, Perkin Elmer AA700) [15] and MB was analyzed by UV-visible spectrophotometer (Shimadzu UV-2550) at 667 nm [10]. The analysis for Pb(II) and MB in binary solutions was performed by dilution 100 times.

2.6. Fixed-bed column data analysis

Adsorption quantities and capacities are important performance indices in column test. Usually, researchers used breakthrough curve to show the performance of adsorbent in the fixed-bed column [11]. Breakthrough curve is expressed in term of C_t/C_0 as a function of time for a given condition, where C_t is the concentration of influent, C_0 is the concentration of effluent [11]. The adsorption capacity of adsorbent under certain operation conditions could be calculated from the breakthrough curve. Breakthrough point is the point that effluent concentration (C_t) reaches about 0.1% of the influent concentration (C_0). The time corresponding is breakthrough time (t_b). When the effluent concentration reaching 95% of the influent concentration, it is exhaustion point, and the time is exhaustion time (t_e) [11]. The total mass of adsorbates adsorbed on GO-sand, q_{total} (mg), could be calculated by the following Eq. (1) [12]:

$$q_{total} = \frac{Q \cdot A}{1000} = \frac{Q}{1000} \int_{t=0}^{t=t_{total}} C_{ad}\, dt \quad (1)$$

where t_{total} is the total flow time (min), Q is the flow rate (mL/min) and A is the area above the breakthrough curve, C_{ad} (mg/L) is the adsorbed concentration.

The total amount of adsorbates flow through the column is calculated by Eq. (2) [11]:

$$m_{total} = \frac{C_0 \cdot Q \cdot t_{total}}{1000} \quad (2)$$

The equilibrium uptake q_{eq} (mg/g) or maximum capacity of the column in the column is calculated by Eq. (3) [11]:

$$q_{eq} = \frac{q_{total}}{m} \quad (3)$$

where m is the dry weight of adsorbent in the column (g).

2.7. Modeling of column data

In previous papers, several mathematical models were utilized to describe and analyze the column studies. Salman et al. [24] used Adams–Bohart model, Thomas model and Yoon–Nelson model to determine the model that best describes the kinetics of the adsorption of 2,4-dichlorophenoxyacetic acid onto activated carbon derived from oil palm frond (PFAC) in the column. Khoo et al. [25] applied the Thomas, Belter and Chu, and bed-depth service time (BDST) model to fit the sorption data and found that Chu model agreed well with the experimental values for all the dye systems. In this work, Yoon–Nelson model was established to fit the experimental data.

3. Results and discussion

3.1. Characterization of adsorbents

XPS could help us to identify the functional groups and elements on the surface of adsorbents [26]. Fig. 2 shows the XPS wide-scan of GO-sand before and after uptake by Pb(II) and MB, respectively. It occurred Pb(II) peak (at 138.32 and 143.54 eV, see the inset in Fig. 2b), demonstrating that Pb(II) was adsorbed on the surface of GO-sand after Pb(II) uptake. It can also be observed that the emerging of N1s peak (at 399.98 eV, see the inset in Fig. 2c), indicating that MB had been successfully adsorbed on the surface of GO-sand.

Fig. 3a shows the high-resolution C1s XPS spectrum of GO-sand before uptake by Pb(II) and MB. It was resolved into three peaks, which located at 284.58, 286.58 and 288.18 eV representing graphic carbon (C—C), carbon present in alcohol (C—OH) and carboxyl groups (O—C═O), respectively [10]. Obviously, in Fig. 3b, the atomic percentage (at.%) of C—O group decreased from 37.53 to 28.36 after uptake by Pb(II) indicating that hydroxyl carbon took part in the adsorption of Pb(II). According to Fig. 3d, only one peak (at 531.98 eV, carboxyl group (C═O)) existed in the high-resolution O1s XPS spectra of GO-sand before uptake by Pb(II) and MB. [26]. In addition, another peak occurred at 530.48 eV (see Fig. 4e) after GO-sand uptake by Pb(II), which may be caused by Pb(II) adsorption on the surface of adsorbent in the form of PbO or Pb—O—R (R represents functional groups) [26]. Furthermore, the Pb $4f_{7/2}$ peak at 138.32 eV was assigned to PbO (see the inset in Fig. 2b), which was consistent with the O1s XPS spectra [26].

The atomic percentage of N shown in Table 1 increased from 1.08 to 2.65, which indicated that MB adsorbed on the surface of GO-sand successfully. Tamez Uddin et al. [6] analyzed the functional groups on surface of jackfruit (*Artocarpus heteropyllus*) leaf powder using FTIR for adsorption MB in fixed-bed column. They found that OH, COOH and CO groups on jackfruit surface were the sorption sites for interaction with dye molecules. As seen from Fig. 3c, it was clear that C—O and C═O groups before and after MB uptake by GO-sand decreased from 37.53 at.% and 10.34 at.% to 31.76 at.% and 6.87 at.%, respectively.

3.2. Adsorption of Pb(II) and MB in fixed-bed column for single solution

3.2.1. Comparison of adsorption capacity of several adsorbents

The column tests packed with sand alone and GO-sand were conducted at given conditions of flow rate (2 mL/min), bed depth (15 cm), and fixed concentration of Pb(II) (200 mg/L) and MB (100 mg/L) influents at pH 4.10 and 4.21 separately. The results were shown in Table 2. It was observed that the total flow time of Pb(II) and MB in sand filter was 180 min and 270 min, respectively. However, compared with that in sand alone, the total flow time increased greatly in GO-sand, which was 400 min and 680 min

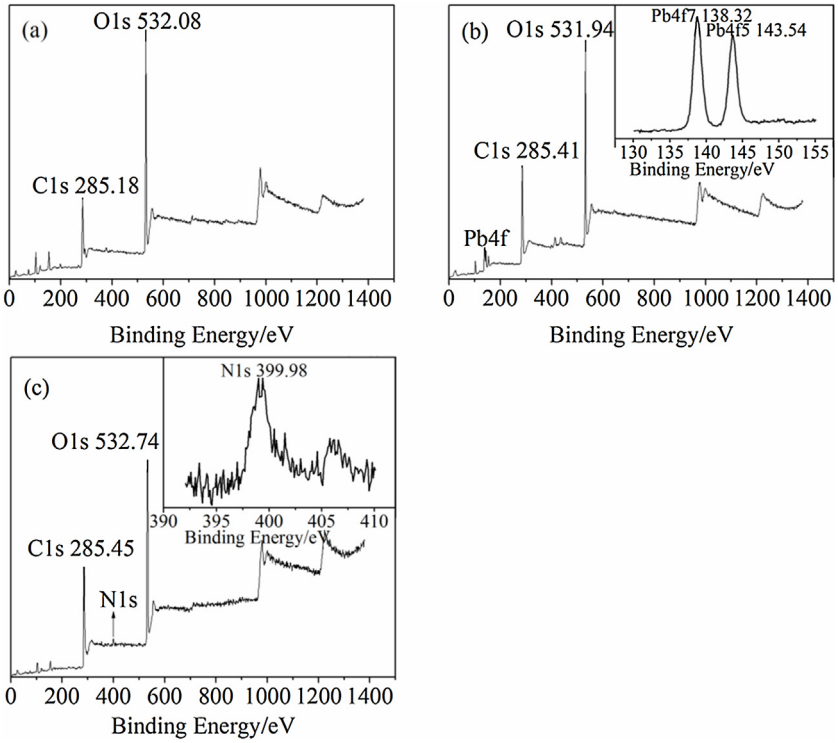

Fig. 2. XP survey spectra: survey of GO-sand (a), survey of GO-sand uptake by Pb(II) (b), and survey of GO-sand uptake by MB (c).

for Pb(II) and MB, respectively. It was suggested that GO-sand filter was much more favorable to Pb(II) and MB uptake when compared to that for sand filter in fixed-bed columns. Furthermore, compared with sand filter, both the total mass of adsorbates (q_{total}) and the equilibrium uptake (q_{eq}) for GO-sand filter was greatly increased (listed in Table 2). Results showed that q_{total} and q_{eq} of GO-sand filter was more than 10 times sand filter for both Pb(II) and MB uptake. Furthermore, the maximum adsorption capacity of GO-sand filter toward Pb(II) (0.63 mg/g) was much higher than previous reported adsorbents, such as algae *Gelidium* (0.083 mg/g) [27], dye loaded coir fiber (0.020 mg/g) [28], functionalized SBA-15 mesoporous silica with polyamidoamine groups (0.269 mg/g) [29] and activated tea waste (0.497 mg/g) [30]. In addition, the maximum adsorption capacity of GO-sand filter toward MB (0.74 mg/g) was much higher

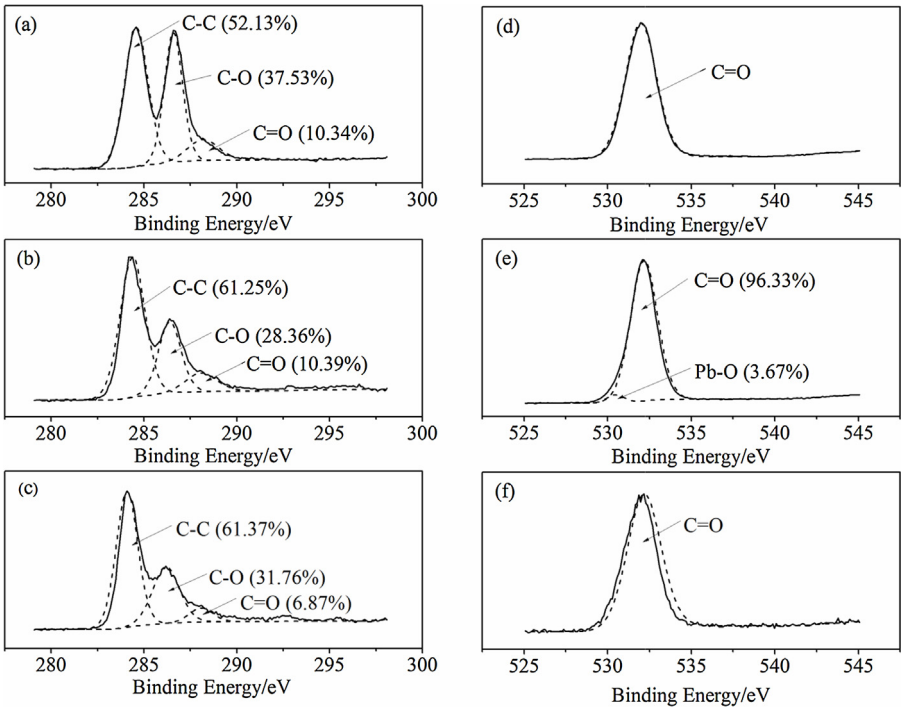

Fig. 3. C1s and O1s spectra: C1s of GO-sand (a), C1s of GO-sand uptake by Pb(II) (b), C1s of GO-sand uptake by MB (c), O1s of GO-sand (d), O1s of GO-sand uptake by Pb(II) (e), and O1s of GO-sand uptake by MB (f).

Table 1
Percentage of atom of GO-sand before and after uptake by Pb(II) and MB.

Elements	GO-sand		GO-sand uptake by Pb(II)		GO-sand uptake by MB	
	Binding energy (eV)	Atomic (%)	Binding energy (eV)	Atomic (%)	Binding energy (eV)	Atomic (%)
C1s	285.18	46.18	285.41	59.40	285.45	59.17
O1s	532.08	52.53	531.94	38.74	532.74	37.97
N1s	400.78	1.08	398.50	1.20	399.98	2.65
$Pb4f_{5/2}$	–	–	143.54	0.21	–	–
$Pb4f_{7/2}$	–	–	138.32	0.23	–	–
Cl2s	269.30	0.14	270.08	0.14	269.42	0.13
S2s	229.37	0.07	228.43	0.08	231.08	0.07

Table 2
Column data in fixed-bed column for Pb(II) and MB adsorption in single and binary solutions.

	Pb(II)			MB		
	t_{total} (min)	q_{total} (mg)	q_{eq} (mg/g)	t_{total} (min)	q_{total} (mg)	q_{eq} (mg/g)
Sand/single solution	180	4.00	0.05	270	5.31	0.07
GO-sand/single solution	400	46.83	0.63	680	55.33	0.74
GO-sand/binary solution	220	26.97	0.36	780	71.50	0.95

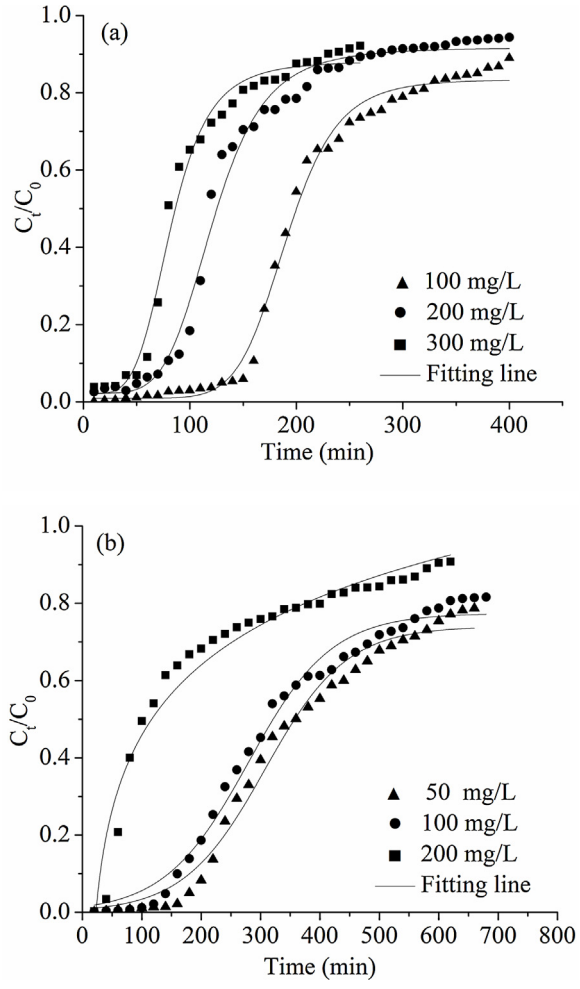

Fig. 4. Breakthrough curves of heavy metal ion and dye in fixed-bed column packed with GO-sand at different initial concentration: (a) for Pb(II) (bed depth = 15 cm, pH 4.10, flow rate = 2 mL/min, C_0: ▲ 100 mg/L, ● 200 mg/L, ■ 300 mg/L) and (b) for MB (bed depth = 15 cm, pH 4.21, flow rate = 2 mL/min, C_0: ▲ 50 mg/L, ● 100 mg/L, ■ 200 mg/L). Symbols: experimental data, solid lines: predictions of the Yoon–Nelson model.

than previous reported adsorbent such as cotton-alk (0.024 mg/g) [31].

3.2.2. *Effect of initial concentration*

Fig. 4 shows the breakthrough curves of Pb(II) and MB at different initial concentrations. It was obvious that the breakthrough curves became sharper, breakthrough time and exhaustion points became shorter with increasing concentration of Pb(II) and MB. This result was similar to that reported in previous studies. Chen et al. [11] investigated the effect of influent Cr(VI) concentration on breakthrough curves and found that a decrease in Cr(VI) concentration obtained a later breakthrough curve. The tendency was also obtained by Bulgariu et al. [32]. They observed that when the initial Pb(II) concentration was higher, breakthrough and saturation were obtained earlier and the breakthrough curves were steeper. In terms of MB adsorption in column tests, Han et al. [3] also discovered that breakthrough time decreased and sharper breakthrough curves were obtained with increasing influent MB concentration. Foo et al. [33] also concluded that breakthrough time decreased and the slope of breakthrough curves increased when influent MB concentration increased. These results can be explained that more adsorption sites were covered with increasing MB concentration [3]. Table 4 shows that the adsorption quantity of Pb(II) increases at higher concentration and the adsorption quantity of MB reaches largest at the concentration of 100 mg/L.

3.2.3. *Effect of bed depth*

The effect of bed depth (10, 15 and 20 cm) on the adsorption of Pb(II) and MB in column tests was investigated under a given condition. The detailed experimental parameters were shown in Table 4. Results showed that the adsorption quantities and capacities of both Pb(II) and MB increased with increasing bed depth. It was observed that (see Fig. 5) that the slope of breakthrough curves decreased and the adsorption process reached saturation slower with increasing bed depth. These results may be due to a longer contact time caused by more adsorbent in the fixed-bed column, which provided more binding sites and larger surface for the removal of Pb(II) and MB [6,11]. Similar tendency was also reported by Salman et al. for 2,4-dichlorophenoxyacetic acid adsorption in a fixed-bed column packed with activated carbon derived from oil palm frond (PFAC) [24]. They concluded that the breakthrough time, exhaustion time and bed capacity increased as bed depth increased [24].

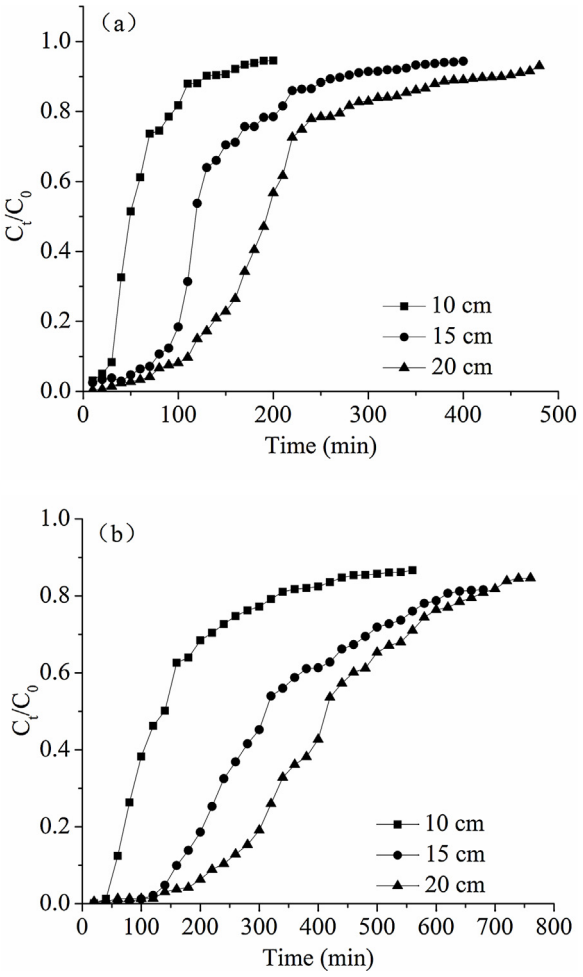

Fig. 5. Breakthrough curves of heavy metal ion and dye in fixed-bed column packed with GO-sand at different bed depth: (a) for Pb (C_0 = 200 mg/L, pH 4.10, flow rate = 2 mL/min, bed depth: ■ 10 cm; ● 15 cm; ▲ 20 cm) and (b) for MB (C_0 = 100 mg/L, pH 4.21, flow rate = 2 mL/min, bed depth: ■ 10 cm; ● 15 cm; ▲ 20 cm).

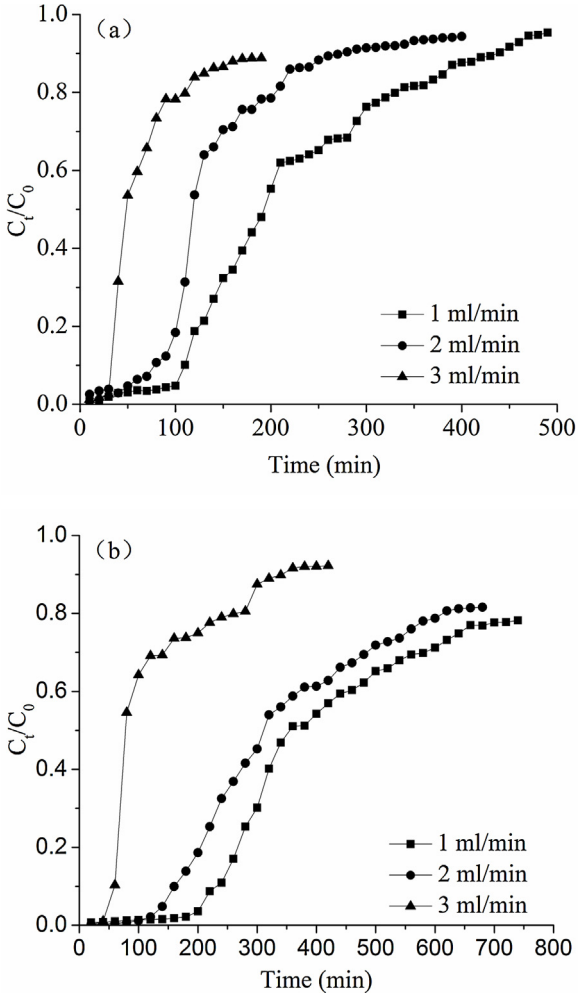

Fig. 6. Breakthrough curves of heavy metal ion and dye in fixed-bed column packed with GO-sand at different flow rate: (a) for Pb(II) (bed depth = 15 cm, pH 4.10, C_0 = 200 mg/L, flow rate: ■ 1 mL/min; ● 2 mL/min; ▲ 3 mL/min) and (b) for MB (bed depth = 15 cm, pH 4.21, C_0 = 100 mg/L, flow rate: ■ 1 mL/min; ● 2 mL/min; ▲ 3 mL/min).

3.2.4. *Effect of flow rate*

The effect of flow rate was investigated at the flow rate of 1, 2 and 3 mL/min. As seen from Fig. 6, for both Pb(II) and MB, sharper breakthrough curves were obtained with increasing flow rate. As the flow rate increased from 1 to 3 mL/min, the exhaustion time of Pb(II) and MB shown in Table 3 decreased from 490 min to 190 min and from 740 min to 420 min, respectively. It was seen that adsorption quantities and capacities also decreased with increasing flow rate. This phenomenon was due to that the residence time of adsorbate in column decreased at high flow rate [24,34] and adsorbate would leave the column before the adsorption equilibrium because of insufficient residence time [6,34].

3.2.5. *Effect of pH*

The value of pH plays an important role in the adsorption process. Previous study proved that lead hydroxide began to form precipitation at the pH value above 6.0 [35]. Herein, the pH of Pb(II) influent solution in this work was less than 6.0. However, MB had a wide range of pH and Tamez Uddin et al. [6] investigated the effect of pH ranging from 3 to 10 on MB adsorption in fixed-bed column.

It can be seen from Fig. 7 that the slope of breakthrough curves at lower pH value was steeper than that at higher pH value. Table 3 shows that the adsorption quantities and capacities increased with increasing pH value. Researchers had reported that competition between cationic and hydrogen ions occurred at low pH for binding on the surface of adsorbent [35]. The similar shapes of breakthrough curves were obtained by Han et al., they used chaff as adsorbent in fixed-bed column for the removal of copper (II) and lead (II) and found that the breakthrough curves shifted from left to right, reaching saturation would spend more time and the adsorption capacity increased with increasing pH [36]. Tamez Uddin et al. [6] also investigated the effect of pH on MB adsorption in a fixed-bed column study. They observed that the time reaching saturation would be longer at higher pH and adsorption quantities and capacities increased with increasing pH value (Fig. 8).

3.3. *Adsorption of Pb(II) and MB in fixed-bed column for binary solution*

To investigate the effect of co-pollutants (i.e. metal ion and dye binary) behavior in a fixed-bed column, binary solution containing both Pb(II) and MB was prepared as influent solution under given conditions (for Pb(II), 15 cm bed depth, 2 mL/min flow rate, 200 mg/L concentration and pH 4.10; and for MB, 15 cm bed depth, 2 mL/min flow rate, 100 mg/L concentration and pH 4.21).

The results were listed in Table 2. It is obvious that for Pb(II) adsorption in binary solution in column test, the exhaustion time

Table 3
Column data and parameters in fixed-bed column for Pb(II) and MB adsorption by GO-sand.

Ion	C_0 (mg/L)	Q (mL/min)	Z (cm)	pH	t_{total} (min)	q_{total} (mg)	q_{eq} (mg/g)
Pb(II)	100	2	15	4.10	400	38.15	0.51
	200	2	15	4.10	400	46.83	0.63
	300	2	15	4.10	260	46.86	0.63
	200	2	10	4.10	200	19.12	0.38
	200	2	15	4.10	400	46.83	0.63
	200	2	20	4.10	480	75.67	0.76
	200	1	15	4.10	490	53.25	0.71
	200	2	15	4.10	400	46.83	0.63
	200	3	15	4.10	190	27.51	0.37
	200	2	15	3.19	180	22.20	0.30
	200	2	15	4.10	400	46.83	0.63
	200	2	15	4.93	460	80.65	1.08
MB	50	2	15	4.21	660	29.99	0.40
	100	2	15	4.21	680	55.33	0.74
	200	2	15	4.21	620	36.50	0.49
	100	2	10	4.21	560	22.55	0.45
	100	2	15	4.21	680	55.33	0.74
	100	2	20	4.21	760	79.61	0.80
	100	1	15	4.21	740	61.79	0.82
	100	2	15	4.21	680	55.33	0.74
	100	3	15	4.21	420	22.85	0.30
	100	2	15	2.51	400	16.58	0.22
	100	2	15	4.21	680	55.33	0.74
	100	2	15	8.66	780	71.61	0.96

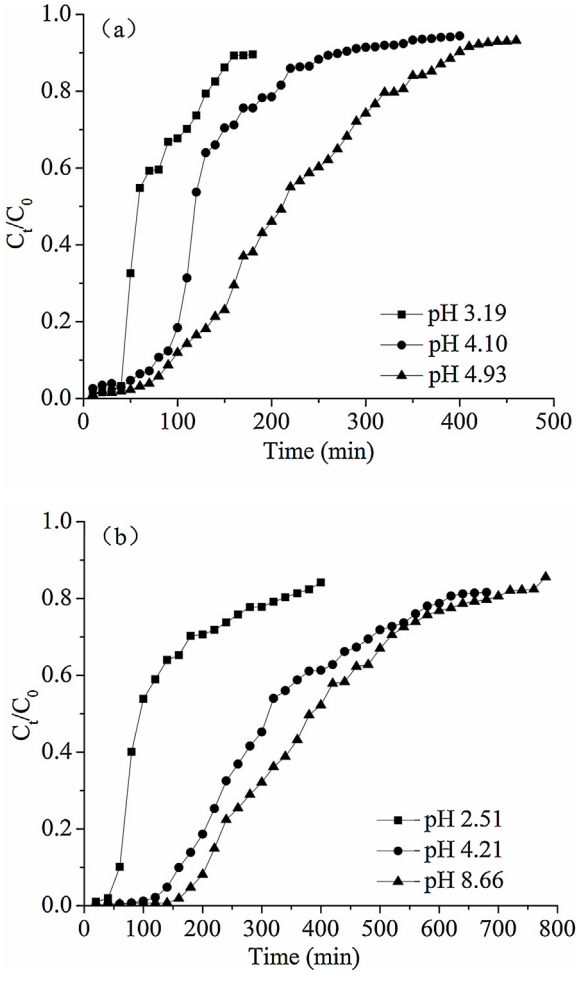

Fig. 7. Breakthrough curves of heavy metal ion and dye in fixed-bed column packed with GO-sand at different pH: (a) for Pb(II) (bed depth = 15 cm, C_0 = 200 mg/L, flow rate = 2 mL/min, pH: ■ 3.19; ● 4.10; ▲ 4.93) and (b) for MB (bed depth = 15 cm, C_0 = 100 mg/L, flow rate = 2 mL/min, pH: ■ 2.51; ● 4.21; ▲ 8.66).

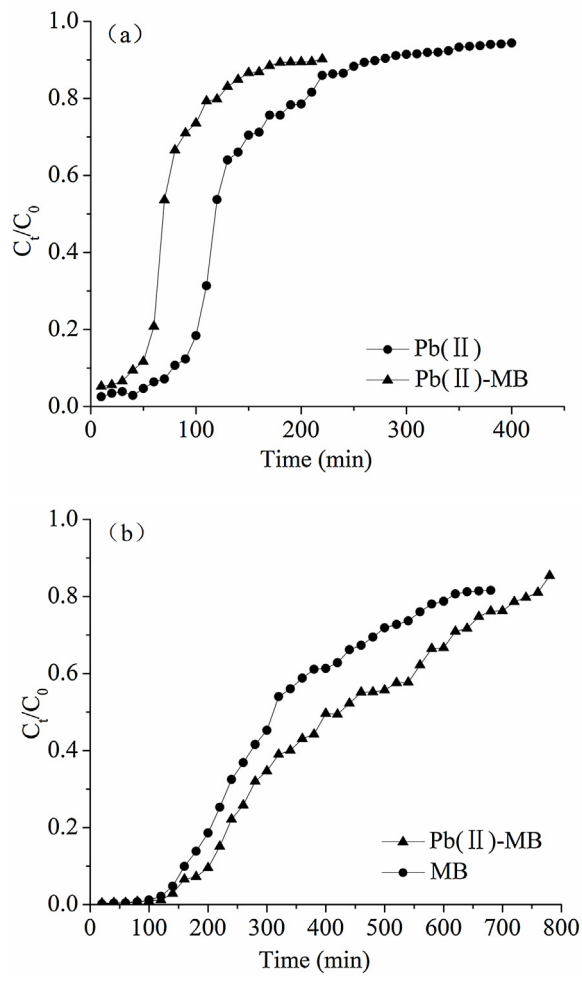

Fig. 8. Breakthrough curves of comparison between single and binary solutions in fixed-bed column packed with GO-sand: (a) for Pb(II) (bed depth = 15 cm, pH 4.10, flow rate = 2 mL/min, C_0 = 200 mg/L) and (b) for MB (bed depth = 15 cm, pH 4.21, flow rate = 2 mL/min, C_0 = 100 mg/L).

Table 4
Adams–Bohart fitting parameters for the adsorption of Pb(II) and MB.

	Concentration (mg/L)	k_{AB} (10^{-2})	N_0 (mg/L)	R^2
Pb(II)	100	1.550	13.511	0.834
	200	0.451	24.579	0.672
	300	0.324	33.864	0.682
MB	50	0.887	855.736	0.831
	100	0.379	1750.247	0.804
	200	0.095	2994.832	0.613

Table 5
Thomas fitting parameters for the adsorption of Pb(II) and MB.

	Concentration (mg/L)	$k_{Th} \times 10^{-2}$	q_{Th} (mg/g)	R^2
Pb(II)	100	2.213	6.526	0.949
	200	0.91	8.401	0.954
	300	0.614	12.196	0.928
MB	50	1.163	11.763	0.942
	100	0.526	22.749	0.939
	200	0.180	22.135	0.804

decreased from 400 to 220 min, and both adsorption quantities and capacities also decreased. The reason can be explained by the more favorable adsorption for MB onto the surface of GO-sand than that for Pb(II), which was derived from π–π interaction between MB and GO on sand surface in packed filter. On the contrary, for MB adsorption in binary solution in column test, the exhaustion time was increased from 680 to 780 min, and both adsorption quantities and capacities were also enhanced. It might be explained by the presence of π–π conjugated electrons in complex, which could donate electron to enhance the electron density on S atom to form stable complexes with the heavy metals [9].

3.4. Breakthrough curve modeling

3.4.1. Adams–Bohart model

Adams–Bohart model was established by Bohart and Adams, which was based on the surface reaction theory and described the relationship between C_t/C_0 and column service time (t) for purification in a flowing system. The expression is as Eq. (4):

$$\ln\left(\frac{C_t}{C_0}\right) = k_{AB}C_0 t - k_{AB}N_0\left(\frac{Z}{F}\right) \quad (4)$$

where k_{AB} (L/mg min) and N_0 (mg/L) are the adsorption rate constant and the saturation concentration, respectively. Z (cm) is the bed depth and F is the ratio of the Q (cm^3/min) to the column sectional area (cm^2). The parameters of $k_{AB}C_0$ and $k_{AB}N_0(Z/F)$ can be calculated from the intercept and slope of the linear plot of $\ln(C_t/C_0)$ against t (not shown by figure).

The experimental data of breakthrough curves for Pb(II) and MB were fitted to the Adams–Bohart model with different initial concentration and listed in Table 4, along with the correlation coefficients (R^2). From Table 4, both for Pb(II) and MB, the predicted values of k_{AB} decreased with increasing the initial concentration, indicating that overall system kinetics was dominated by external mass transfer in the initial part of adsorption in the column [11,37].

3.4.2. Thomas model

The Thomas model [38] is a widely used theoretical method to describe the column performance, which assumes plug flow behavior in the bed. The linearized form of Thomas model can be expressed as Eq. (5):

$$\ln\left(\frac{C_0}{C_t}\right)(-1) = \frac{k_{Th}q_0 m}{Q} - k_{Th}C_0 t \quad (5)$$

where k_{Th} (mL/min mg) is the Thomas model constant, q_0 (mg/g) is the adsorption capacity. The values of k_{Th} and q_0 can be determined from the linear plot of $\ln[(C_0/C_t) - 1]$ against t (not shown by figure).

The experimental data of breakthrough curves for Pb(II) and MB were fitted to the Thomas model with different initial concentration and listed in Table 5. It was shown that the Thomas model provided a better fitting compared to Adams–Bohart model. According to Table 5, it can be seen that with the initial concentration increasing, the k_{Th} decreased while the value of q_0 increased for Pb(II) and MB. It was attributed to the driving force for adsorption in the concentration difference. The Thomas model was suitable for adsorption processes where the external and internal diffusions were not the limiting step [3,39].

Table 6
Comparison between the parameters of Yoon–Nelson model and experimental data.

	Concentration (mg/L)	τ (min)		k_{YN} (10^{-2})		R^2
		Exp	Cal	Exp	Cal	
Pb(II)	100	216	249	2.098	2.173	0.993
	200	134	167	2.716	1.716	0.989
	300	96	118	3.056	2.373	0.986
MB	50	402	439	0.771	1.167	0.986
	100	363	418	0.756	1.072	0.987
	200	150	212	0.719	0.704	0.958

3.4.3. Yoon–Nelson model

Yoon–Nelson model was established by Yoon and Nelson in 1984 [11], which based on the assumption that the rate of decrease in the probability of adsorption for each adsorbate molecule was proportional to the probability of adsorbate adsorption and the probability of adsorbate breakthrough on the adsorbent [39]. It is a simple model and does not require detailed data about the characteristics of adsorbate, the type of adsorbent, and the physical properties of the adsorption bed [40]. It is a model for a single component system, the linearized equation of model expressed as Eq. (6): [39]

$$\ln\left(\frac{C_t}{C_0 - C_t}\right) = k_{YN}t - \tau k_{YN} \quad (6)$$

where k_{YN} (min^{-1}) is the rate of constant and τ (min) is the time required 50% adsorbate breakthrough. Linear fitting lines were shown in Fig. 9. The parameters of k_{YN} and τ can be calculated from the intercept and slope of the linear plot of $\ln[C_t/(C_0 - C_t)]$ against t.

The experimental data of breakthrough curves for Pb(II) and MB were fitted to the model with different initial concentration. Fig. 5 shows the fitting breakthrough graphs of Pb(II) and MB. Obviously, it appeared a good fitting between the experimental points and predicted normalized concentration. The values of k_{YN} and τ obtained from experimental and calculated were shown in Table 6. Obviously, as initial concentration increased, for Pb(II), the value of τ decreased and k_{YN} increased. However, for MB, τ and k_{YN} values decreased with increasing influent concentration. The value of τ decreased as the initial concentration increased, because the saturation of the column occurred more quickly [40]. As initial concentration increasing, the force that control mass transfer in liquid phase increased could explain the increase of k_{YN} [41]. In a comparison of values of R^2, both the Thomas and Yoon–Nelson models can be used to predict adsorption performance for adsorption of Pb(II) and MB in a fixed-bed column.

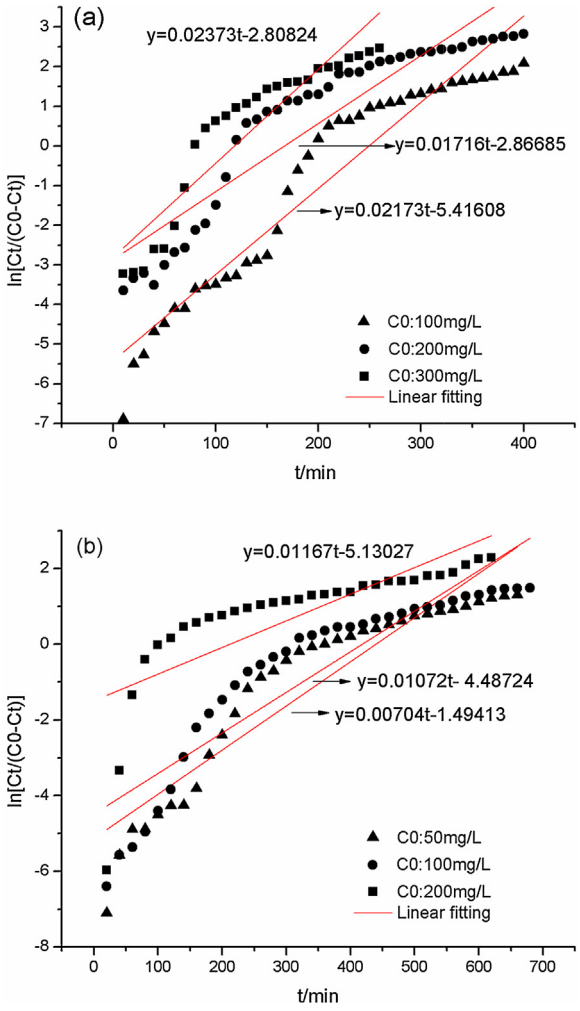

Fig. 9. The linear fitting of $\ln[C_t/(C_0 - C_t)]$ against t of Yoon–Nelson model for Pb(II) (a) and MB (b).

4. Conclusion

This study demonstrated that GO-sand as a low-cost filter was an effective adsorbent for the removal of Pb(II) and MB in fixed-bed column. XPS analysis illustrated that Pb(II) and MB were successfully uptaken by GO-sand filter in column tests. Results showed that q_{total} and q_{eq} of GO-sand filter was more than 10 times sand filter for both Pb(II) and MB uptake. The experimental parameters were discussed in detail including initial concentration, bed depth, flow rate and influent solution pH. Adsorption quantities and capacities increased with increasing initial concentration, bed depth and influent solution pH, but decreased with increasing flow rate. Noticeably, Pb(II) adsorption was suppressed, but MB uptake was enhanced in Pb(II)–MB binary solution in fixed-bed column. The experimental data of breakthrough curves for both Pb(II) and MB were well described by Yoon–Nelson model.

Acknowledgments

This work is financially supported by the National Natural Science Foundation of China (Grant nos. 51039001, 51378190, 50808070, 51108166, 21275044), the Program for Changjiang Scholars and Innovative Research Team in University (IRT-13R17), the Interdisciplinary Research Funds for Hunan University (Grant no. 531107040761), the Scientific Research Foundation for the Returned Overseas Chinese Scholars (Grant no. 2013693), and the Natural Science Foundation of Hunan Province, China (Grant no. 12JJB003).

References

[1] A. Shahbazi, H. Younesi, A. Badiei, Functionalized SBA-15 mesoporous silica by melamine-based dendrimer amines for adsorptive characteristics of Pb(II), Cu(II) and Cd(II) heavy metal ions in batch and fixed bed column, Chem. Eng. J. 168 (2011) 505–518.
[2] O. Olanipekun, A. Oyefusi, G.M. Neelgund, A. Oki, Adsorption of lead over graphite oxide, Spectrochim. Acta A 118 (2014) 857–860.
[3] R.P. Han, Y. Wang, X. Zhao, Y.F. Wang, F.L. Xie, J.M. Cheng, M.S. Tang, Adsorption of methylene blue by phoenix tree leaf powder in a fixed-bed column: experiments and prediction of breakthrough curves, Desalination 245 (2009) 284–297.
[4] N. Atar, A. Olgun, S.B. Wang, S.M. Liu, Adsorption of anionic dyes on boron industry waste in single and binary solutions using batch and fixed-bed systems, J. Chem. Eng. Data 56 (2011) 508–516.
[5] M. Ghaedi, N. Zeinali, A.M. Ghaedi, M. Teimuori, J. Tashkhourian, Artificial neural network-genetic algorithm based optimization for the adsorption of methylene blue and brilliant green from aqueous solution by graphite oxide nanoparticle, Spectrochim. Acta A 125 (2014) 264–277.
[6] Md. Tamez Uddin, Md. Rukanuzzaman, Md. Maksudur Rahman Khan, Md. Akhtarul Islam, Adsorption of methylene blue from aqueous solution by jackfruit (*Artocarpus heteropyllus*) leaf powder: a fixed-bed column study, J. Environ. Manage. 90 (2009) 3443–3450.
[7] M. Visa, Tailoring fly ash activated with bentonite as adsorbent for complex wastewater treatment, Appl. Surf. Sci. 263 (2012) 753–762.
[8] V. Hernández-Montoya, M.A. Pérez-Cruz, D.I. Mendoza-Castillo, M.R. Moreno-Virgen, A. Bonilla-Petriciolet, Competitive adsorption of dyes and heavy metals on zeolitic structures, J. Environ. Manage. 116 (2013) 213–221.
[9] M. Visa, A.M. Chelaru, Hydrothermally modified fly ash for heavy metals and dyes removal in advanced wastewater treatment, Appl. Surf. Sci. 303 (2014) 14–22.
[10] J.H. Deng, X.R. Zhang, G.M. Zeng, J.L. Gong, Q.Y. Niu, J. Liang, Simultaneous removal of Cd(II) and ionic dyes from aqueous solution using magnetic graphene oxide nanocomposite as an adsorbent, Chem. Eng. J. 226 (2013) 189–200.
[11] S.H. Chen, Q.Y. Yue, B.Y. Gao, Q. Li, X. Xu, K.F. Fu, Adsorption of hexavalent chromium from aqueous solution by modified corn stalk: a fixed-bed column study, Bioresour. Technol. 113 (2012) 114–120.
[12] R.P. Han, L.N. Zou, X. Zhao, Y.F. Xu, F. Xu, Y.L. Li, Y. Wang, Characterization and properties of iron oxide-coated zeolite as adsorbent for removal of copper(II) from solution in fixed bed column, Chem. Eng. J. 149 (2009) 123–131.
[13] L.L. Fan, C.N. Luo, M. Sun, X.J. Li, H.M. Qiu, Highly selective adsorption of lead ions by water-dispersible magnetic chitosan/graphene oxide composites, Colloids Surf. B 103 (2013) 523–529.
[14] G.D. Vuković, A.D. Marinković, S.D. Škapin, M.Đ. Ristić, R. Aleksić, A.A. Perić-Grujić, P.S. Uskoković, Removal of lead from water by amino modified multi-walled carbon nanotubes, Chem. Eng. J. 173 (2011) 855–865.
[15] M. Machida, T. Mochimaru, H. Tatsumoto, Lead(II) adsorption onto the graphene layer of carbonaceous materials in aqueous solution, Carbon 44 (2006) 2681–2688.
[16] S.T. Yang, S. Chen, Y.L. Chang, A.N. Cao, Y.F. Liu, H.F. Wang, Removal of methylene blue from aqueous solution by graphene oxide, J. Colloid Interface Sci. 359 (2011) 24–29.
[17] M.F. Zhao, P. Liu, Adsorption of methylene blue from aqueous solutions by modified expanded graphite powder, Desalination 249 (2009) 331–336.
[18] S. Stankovich, D.A. Dikin, G.H. Dommett, K.M. Kohlhaas, E.J. Zimney, E.A. Stach, R.D. Piner, S.T. Nguyen, R.S. Ruoff, Graphene-based composite materials, Nature 442 (2006) 282–286.
[19] S.M. Lee, C. Laldawngliana, D. Tiwari, Iron oxide nano-particles-immobilized-sand material in the treatment of Cu(II), Cd(II) and Pb(II) contaminated waste waters, Chem. Eng. J. 195 (2012) 103–111.
[20] A. Eisazadeh, H. Eisazadeh, K.A. Kassim, Removal of Pb(II) using polyaniline composites and iron oxide coated natural sand and clay from aqueous solution, Synth. Met. 171 (2013) 56–61.
[21] J. Mähler, I. Persson, Rapid adsorption of arsenic from aqueous solution by ferrihydrite-coated sand and granular ferric hydroxide, Appl. Geochem. 37 (2013) 179–189.
[22] W.S. Hummers, J.R.E. Offman, Preparation of graphitic oxide, J. Am. Chem. Soc. 80 (1958) 1339.
[23] W. Gao, M. Majumder, L.B. Alemany, T.N. Narayanan, M.A. Ibarra, B.K. Pradhan, P.M. Ajayan, Engineered graphite oxide materials for application in water purification, ACS Appl. Mater. Interfaces 3 (2011) 1821–1826.
[24] J.M. Salman, V.O. Njoku, B.H. Hameed, Batch and fixed-bed adsorption of 2,4-dichlorophenoxyacetic acid onto oil palm frond activated carbon, Chem. Eng. J. 174 (2011) 33–40.
[25] E.C. Khoo, S.T. Ong, S.T. Ha, Removal of basic dyes from aqueous environment in single and binary systems by sugarcane bagasse in a fixed-bed column, Desalin. Water Treat. 37 (2012) 215–222.
[26] H.J. Wang, A.L. Zhou, F. Peng, H. Yu, J. Yang, Mechanism study on adsorption of acidified multiwalled carbon nanotubes to Pb(II), J. Colloid Interface Sci. 316 (2007) 277–283.

[27] A. Shahbazi, H. Younesi, A. Badiei, Batch and fixed-bed column adsorption of Cu(II), Pb(II) and Cd(II) from aqueous solution onto functionalised SBA-15 mesoporous silica, Can. J. Chem. Eng. 91 (2013) 739–750.
[28] M.K. Mondal, Removal of Pb(II) ions from aqueous solution using activated tea waste: adsorption on a fixed-bed column, J. Environ. Manage. 90 (2009) 3266–3271.
[29] V.J. Vilar, J.M. Loureiro, C.M. Botelho, R.A. Boaventura, Continuous biosorption of Pb/Cu and Pb/Cd in fixed-bed column using algae gelidium and granulated agar extraction algal waste, J. Hazard. Mater. 154 (2008) 1173–1182.
[30] S.R. Shukla, R.S. Pai, Comparison of Pb(II) uptake by coir and dye loaded coir fibres in a fixed bed column, J. Hazard. Mater. 125 (2005) 147–153.
[31] Z. Ding, X. Hu, A.R. Zimmerman, B. Gao, Sorption and cosorption of lead (II) and methylene blue on chemically modified biomass, Bioresour. Technol. 167 (2014) 569–573.
[32] D. Bulgariu, L. Bulgariu, Sorption of Pb(II) onto a mixture of algae waste biomass and anion exchanger resin in a packed-bed column, Bioresour. Technol. 129 (2013) 374–380.
[33] K.Y. Foo, B.H. Hameed, Dynamic adsorption behavior of methylene blue onto oil palm shell granular activated carbon prepared by microwave heating, Chem. Eng. J. 203 (2012) 81–87.
[34] W.H. Zou, L. Zhao, L. Zhu, Adsorption of uranium(VI) by grapefruit peel in a fixed-bed column: experiments and prediction of breakthrough curves, J. Radioanal. Nucl. Chem. 295 (2013) 717–727.
[35] R.P. Han, W.H. Zou, Z.P. Zhang, J. Shi, J.J. Yang, Removal of copper(II) and lead(II) from aqueous solution by manganese oxide coated sand – I. Characterization and kinetic study, J. Hazard. Mater. 137 (2006) 384–395.
[36] R.P. Han, J.H. Zhang, W.H. Zou, H.J. Xiao, H. Shi, H.M. Liu, Biosorption of copper(II) and lead(II) from aqueous solution by chaff in a fixed-bed column, J. Hazard. Mater. 133 (2006) 262–268.
[37] R. Sharma, B. Singh, Removal of Ni (II) ions from aqueous solutions using modified rice straw in a fixed bed column, Bioresour. Technol. 146 (2013) 519–524.
[38] H.C. Thomas, Heterogeneous ion exchange in a flowing system, J. Am. Chem. Soc. 66 (1944) 1466–1664.
[39] S.S. Baral, N. Das, T.S. Ramulu, S.K. Sahoo, S.N. Das, G. Roy Chaudhury, Removal of Cr(VI) by thermally activated weed *Salvinia cucullata* in a fixed-bed column, J. Hazard. Mater. 161 (2009) 1427–1435.
[40] M. Calero, F. Hernainz, G. Blazquez, G. Tenorio, M.A. Martin-Lara, Study of Cr (III) biosorption in a fixed-bed column, J. Hazard. Mater. 171 (2009) 886–893.
[41] Z. Aksu, F. Gönen, Biosorption of phenol by immobilized activated sludge in a continuous packed bed: prediction of breakthrough curves, Process Biochem. 39 (2004) 599–613.